

# Entanglement Swapping using Continuous Variables

R.E.S.Polkinghorne and T.C.Ralph

*Department of Physics, Faculty of Science,  
The Australian National University,  
ACT 0200 Australia  
E-mail: Timothy.Ralph@anu.edu.au*

(submitted to PRL 22nd October 1998)

## Abstract

We investigate the efficacy with which entanglement can be teleported using a continuous measurement scheme. We show that by using the correct gain for the classical channel the degree of violation of locality that can be demonstrated (using a CH type inequality) is *not* a function of the level of entanglement squeezing used in the teleportation. This is possible because a gain condition can always be chosen such that passage through the teleporter is equivalent to pure attenuation of the input field.

It is remarkable that non-local entanglement can be established between particles that have never interacted directly. Here “non-local” refers to the inability of local hidden variable theories to predict the observed correlations. This “entanglement swapping” [1], [2] may be useful in establishing non-local correlations over very large distances and other applications [3]. Recently Pan et al [4] have demonstrated entanglement swapping of the polarization entanglement created by type II parametric down conversion experimentally. In all discussions and experiments to date discrete measurements and manipulations are made in order to transfer the non-local correlations. For example in the optical experiments, photon coincidences operate photo-current gates. However entanglement swapping is really a special case of teleportation [2] and in work by Vaidman [5] and Braunstein and Kimble [6], schemes for the teleportation of continuous quantum variables have been proposed. In these schemes continuous measurements and manipulations are used. A preliminary experimental demonstration of continuous variable teleportation of a coherent state has recently been presented by Furusawa et al [7]. An important question to ask is; can non-local entanglement be swapped or teleported using a continuous measurement scheme?

In this paper we show explicitly that this can be achieved. This effect represents a completely new way of transferring non-local information. Of particular practical significance is that the conditions for achieving non-local effects are not stringent.

The optical arrangement we will investigate is shown in Fig. 1. It combines the basic arrangement of entanglement swapping [4] with a 2-mode generalization of the continuous

variable teleportation scheme [6]. We consider a non-collinear type II optical parametric oscillator operating at low pump efficiency (OPO1) as our source of entangled photons [8]. In the Heisenberg picture the two outputs,  $A$  and  $B$ , can be decomposed into their horizontal ( $h$ ) and vertical ( $v$ ) linear polarization components by

$$\begin{aligned} A &= A_{(h)} \hat{h} + A_{(v)} \hat{v} \\ B &= B_{(h)} \hat{h} + B_{(v)} \hat{v} \end{aligned} \quad (1)$$

where  $\hat{h}$  and  $\hat{v}$  are orthogonal unit vectors,

$$\begin{aligned} A_{(h,v)} &= A_{0(h,v)} \cosh \chi_1 + B_{0(v,h)}^\dagger \sinh \chi_1, \\ B_{(h,v)} &= B_{0(h,v)} \cosh \chi_1 + A_{0(v,h)}^\dagger \sinh \chi_1, \end{aligned} \quad (2)$$

$A_0$  and  $B_0$  are the vacuum inputs to OPO1, and  $\chi_1$  is its conversion efficiency. We have assumed the bandwidth of the OPO is broad compared to our detection bandwidth and that pump depletion can be ignored. The output state of the combined system in the number state basis is given by

$$\frac{1}{\sqrt{2} \cosh(\chi_1)} \sum_{n=0}^{\infty} (\tanh \chi_1)^n (|n_h, n_v\rangle + |n_v, n_h\rangle) \quad (3)$$

where

$$|n_i, n_j\rangle \equiv |n_i\rangle_A \otimes |n_j\rangle_B \quad (4)$$

and  $n_h$  and  $n_v$  are the photon number in the horizontal and vertical polarizations respectively.

This reduces to the number-polarization entangled state

$$\frac{\chi_1}{\sqrt{2}} (|1_h, 1_v\rangle + |1_v, 1_h\rangle) + |0\rangle \quad (5)$$

for low pump efficiency (i.e  $\chi_1 \ll 1$ ). The state given by Eq 5 violates the Clauser-Horne (CH) type inequality [9]

$$S = \frac{R(\theta_A, \theta_B) - R(\theta_A, \theta'_B) + R(\theta'_A, \theta_B) + R(\theta'_A, \theta'_B)}{R(\theta'_A, -B) + R(-A, \theta_B)} \leq 1 \quad (6)$$

where  $R(\theta_A, \theta_B)$  is the photon coincidence count rate between polarisation  $\theta_A$  of beam  $A$  and  $\theta_B$  of  $B$ , and  $R(\theta_A, -B)$  is the equivalent rate counting both polarisations of beam  $B$ . The maximum violation occurs for  $\theta_A = \pi/8$ ,  $\theta_B = -\pi/4$ ,  $\theta'_A = 3\pi/8$  and  $\theta'_B = 0$ , when  $S \approx 1.21$ . Strong violations of locality have been observed experimentally with such a state [8].

Now we consider teleporting, or swapping the entanglement of, one of the beams ( $B$ ) from our non-local source using a continuous variable method. We will then investigate the correlations between the teleported beam and beam  $A$  and determine under what circumstances they still violate the CH inequality. The teleportation is achieved using a second type II OPO (OPO2). The output beams of OPO2,  $C$  and  $D$ , are given by analogous expressions to those of OPO1 (Eq.1,2). The conversion efficiency of OPO2 is  $\chi_2$ . Beam  $B$  is

split into its two polarizations components ( $B_h$  and  $B_v$ ) at a polarizing beam-splitter (see Fig. 1). Similarly beam  $C$  is split into  $C_h$  and  $C_v$ . The horizontally polarized component of OPO1 ( $B_h$ ) is mixed with the horizontally polarized component from OPO2,  $C_h$ , on a 50:50 beamsplitter. The outputs of the beamsplitter are directed to two homodyne detection systems which measure the phase ( $X^-$ ) and amplitude ( $X^+$ ) quadratures of the field. Similarly  $B_v$  and  $C_v$  are mixed and their quadrature amplitudes detected. The resulting photocurrents are proportional to

$$X_{(h,v)}^\pm = \sqrt{1-\eta} X_{\delta(h,v)}^\pm + \sqrt{\eta/2} (X_{B(h,v)}^\pm \pm X_{C0(h,v)}^\pm \cosh \chi_2 + X_{D0(v,h)}^\pm \sinh \chi_2) \quad (7)$$

where, for example  $X_B^- = i(B - B^\dagger)$  and  $X_B^+ = B + B^\dagger$ . The operators  $X_{\delta(h,v)}^\pm$  come from vacuum modes introduced by losses in the homodyne systems, which are assumed to have efficiencies  $\eta$ . The photo-currents are then amplified and fed-forward to the interferometric modulation systems (IMS) depicted in Fig. 2 which act on the individual polarization components of the second beam from OPO2,  $D_h$  and  $D_v$ . The photocurrents from the detection of the horizontally polarized beams are used to modulate  $D_v$  whilst the photo-currents from the detection of the vertically polarized beams are used to modulate  $D_h$ . The effect of the IMS's are to displace the amplitudes of the beams by coupling in power from local oscillator beams (LO). The coupling is achieved via electro-optic modulators (EOM) in the interferometer arms. Provided the phase shifts ( $\phi_{v,h}$ ) introduced by the EOM's are small, the output of the IMS's ( $D'_h$  and  $D'_v$ ) are given by

$$D'_{(h,v)} = D_{(h,v)} + \bar{E} \phi_{v,h} \quad (8)$$

where  $\bar{E}$  is the coherent amplitude of the LO. In general we have

$$\phi_{v,h}(t) = \int_0^t k^+(u) X_{v,h}^+(t-u) du + \int_0^t k^-(u) X_{v,h}^-(t-u) du \quad (9)$$

where  $k^\pm$  contains various constants of proportionality as well as the time response of the feedforward electronics. However, if we restrict our attention to RF frequencies (relative to the local oscillator) for which the frequency response of the electronics is flat we can set

$$k^\pm(u) = \frac{1}{\sqrt{2}\bar{E}} \lambda^\pm \delta(u) \quad (10)$$

where  $\lambda^\pm$  is the feedforward gain, and so

$$D'_{(h,v)} = D_{(h,v)} + \frac{1}{\sqrt{2}} \lambda^+ X_{v,h}^+ + \frac{1}{\sqrt{2}} \lambda^- X_{v,h}^- \quad (11)$$

Finally the beams are recombined using a polarizing beamsplitter and a half-wave plate is used to rotate horizontal polarizations into vertical and vice versa. The output beam is

$$D' = D'_{(v)} \hat{h} + D'_{(h)} \hat{v} \quad (12)$$

Setting ( $\lambda = -\lambda^+ = i\lambda_-$ ) and assuming unit detection efficiency ( $\eta = 1$ ) we obtain

$$D' = \left( B_{(h)} + (\sinh \chi_2 - \lambda \cosh \chi_2) C_{0h}^\dagger + (\cosh \chi_2 - \lambda \sinh \chi_2) D_{0v} \right) \hat{h} \\ + \left( B_{(v)} + (\sinh \chi_2 - \lambda \cosh \chi_2) C_{0v}^\dagger + (\cosh \chi_2 - \lambda \sinh \chi_2) D_{0h} \right) \hat{v} \quad (13)$$

In the limit of strong squeezing ( $\chi_2 \gg 1$  such that  $\cosh \chi_2 \approx \sinh \chi_2$ ) and unity gain ( $\lambda = 1$ ) beams  $B$  and  $D'$  become equivalent. It is clear that in this limit the beams  $A$  and  $D'$  will violate the CH inequality for conditions under which  $A$  and  $B$  violated it, showing that the non-locality has been teleported. This is shown in Fig. 3 where Eq 6 is evaluated as a function of polarizer angle with beams  $A$  and  $D'$  as inputs, unity gain and 99% squeezing.

Very high levels of squeezing are difficult to achieve so it is important to ascertain what levels of squeezing are required to achieve non-local teleportation. Indeed, if we remain at unity gain, the operating point discussed in Ref. [6] and used by Furusawa et al [7], Fig. 3 also shows that non-locality is lost for squeezing less than about 80%. Surprisingly, though, we are able to recover non-local behavior for low levels of squeezing if we reduce the gain in the feedforward loops. This represents a new and potentially useful operating point.

We can write an analytical relationship between the value of  $S$  that could be obtained from photon correlation measurements of beams  $A$  and  $B$ ,  $S_{A,B}$  and that which could be obtained for the same measurements of beams  $A$  and  $D'$ ,  $S_{A,D'}$  in the limit that  $\chi_1 \ll 1$ . We must calculate photon coincidence count rates between beams  $A$  and  $D'$  such as

$$R(\theta_A, \theta_{D'}) = \langle in | E_{D'}^\dagger(\theta_{D'}) E_A^\dagger(\theta_A) E_A(\theta_A) E_{D'}(\theta_{D'}) | in \rangle \quad (14)$$

where

$$E_A(\theta_A) = A_h \cos \theta_A + A_v \sin \theta_A \\ E_{D'}(\theta_{D'}) = D'_h \cos \theta_{D'} + D'_v \sin \theta_{D'} \quad (15)$$

and  $|in\rangle$  is given by Eq. 5. After some algebra one finds

$$R(\theta_A, \theta_{D'}) = \lambda^2 \eta R(\theta_A, \theta_B) + (N^2 + \lambda^2(1 - \eta))/2 \quad (16)$$

where

$$N = \sinh \chi_2 - \lambda \sqrt{\eta} \cosh \chi_2 \quad (17)$$

Similarly we find

$$R(\theta_A, -_{D'}) = \lambda^2 \eta R(\theta_A, -_B) + (N^2 + \lambda^2(1 - \eta)) \quad (18)$$

and

$$R(-_A, \theta_{D'}) = \lambda^2 \eta R(-_A, \theta_B) + (N^2 + \lambda^2(1 - \eta)) \quad (19)$$

Putting these results together as per Eq. 6 we obtain

$$S_{A,D'} = \frac{\frac{N^2}{\lambda^2} + \eta S_{A,B} + 1 - \eta}{\frac{2N^2}{\lambda^2} + 2 - \eta} \quad (20)$$

Consider first unit detection efficiency ( $\eta = 1$ ). Eq. 20 shows that the non-local correlation is preserved by the teleportation *for any level of squeezing* provided we set

$$\lambda_{op} = \tanh \chi_2 \quad (21)$$

This effect is shown in Fig. 4 where the maximum of  $S_{A,D'}$  is plotted against the feedforward gain,  $\lambda$  for various levels of squeezing. As squeezing is reduced equal violations of locality are still achieved for lower levels of gain. The range of feedforward gains for which non-local teleportation is achieved actually broadens to a maximum value as the squeezing is reduced before narrowing again. The mechanism for this surprising result can be understood by examining the action of the teleporter on an arbitrary, single mode input field,  $a_{in}$ . Under ideal conditions the output field is given by

$$a_{out} = \lambda a_{in} + (\cosh \chi - \lambda \sinh \chi) B_0 - (\lambda \cosh \chi - \sinh \chi) A_0^\dagger \quad (22)$$

Notice that photons are added to the output through the action of the creation operator,  $A_0^\dagger$ . These spurious photons are detrimental to the observation of non-local correlations. However no photons are added to the output if the gain condition  $\lambda_{op} = \tanh \chi$  is chosen as the coefficient of  $A_0^\dagger$  goes to zero. The output is then given by

$$a_{out} = \lambda_{op} a_{in} + \sqrt{1 - \lambda_{op}^2} B_0 \quad (23)$$

Eq.23 is formally equivalent to pure attenuation by a factor  $(1 - \lambda_{op}^2)$ . Thus when the teleporter is operated with this gain the output beam  $D'$  is simply an attenuated version of  $B$ . Because  $S$  is a normalized quantity, determined by a ratio of coincidence counts, attenuation does not reduce it.

What we observe in Fig.4 could be considered a smooth transition between teleportation, when the teleporting OPO has strong squeezing, to continuous variable entanglement swapping, when the teleporting OPO has a conversion efficiency similar to that of the source OPO. The teleportation limit is characterized by the exact reproduction of the state of  $B$  on  $D'$ . The beams  $A$  and  $D'$  are in the same polarization-number entangled state as  $A$  and  $B$  were originally. On the other hand, in the entanglement swapping limit, although every photon in  $D'$  has become polarization entangled with a corresponding photon in beam  $A$  the number entanglement has become strongly diluted. This is due to the effective attenuation which leaves many unpaired photons in beam  $A$ . The joint state of beams  $A$  and  $D'$  is now strongly mixed. This situation has been referred to by some authors as "a posteriori" teleportation [10].

Homodyne detection losses will reduce and, for  $\eta \leq 1/S_{A,B}$ , eventually destroy the non-local effects. At the optimum gain condition (now  $\lambda_{op} = \tanh \chi_2 / \sqrt{\eta}$ ) this means the homodyne detection efficiencies must be better than about 83%. This limit is independent of the amount of squeezing. However, reducing the squeezing of OPO2 increases the effective attenuation at the optimum gain condition and hence reduces the coincidence count rate. As a result longer counting times are required to observe non-locality. This reduction in signal to noise is typical of entanglement swapping and is an unavoidable consequence of operating below unity gain [11]. Never-the-less we believe an experimental demonstration is feasible with current technology. For example with  $\eta = 0.9$  and 50% squeezing ( $\chi_2 = 0.34$ ) we find  $S_{A,D'} = 1.08$  with coincidence count rates reduced to about 10% of their unteleported values.

In summary we have shown that it is possible to teleport the non-local correlations associated with number-polarization entanglement using a continuous variable scheme. The

non-local correlations can be teleported for any level of squeezing in the teleporting OPO (OPO2). In general the best operating point for teleportation of the entanglement is where the output of the teleporter is simply an attenuated version of the input beam. This operating point is clearly of importance for a large range of superposition and entangled state inputs.

We thank S.L.Braunstein for stimulating discussions. This work was supported by the Australian Research Council.

## FIGURES

FIG. 1. Schematic of the teleportation arrangement. OPO1 produces pairs of photons with entangled polarizations in beams A and B. The polarization modes of beam B are separated, and teleported separately into beam D. The squeezed resource is provided by OPO2. The polarization modes are swapped during teleportation, so a half wave plate is inserted to swap them back. Finally, coincidence measurements are taken on modes A and D' to test for violation of the Clauser-Horne inequality.

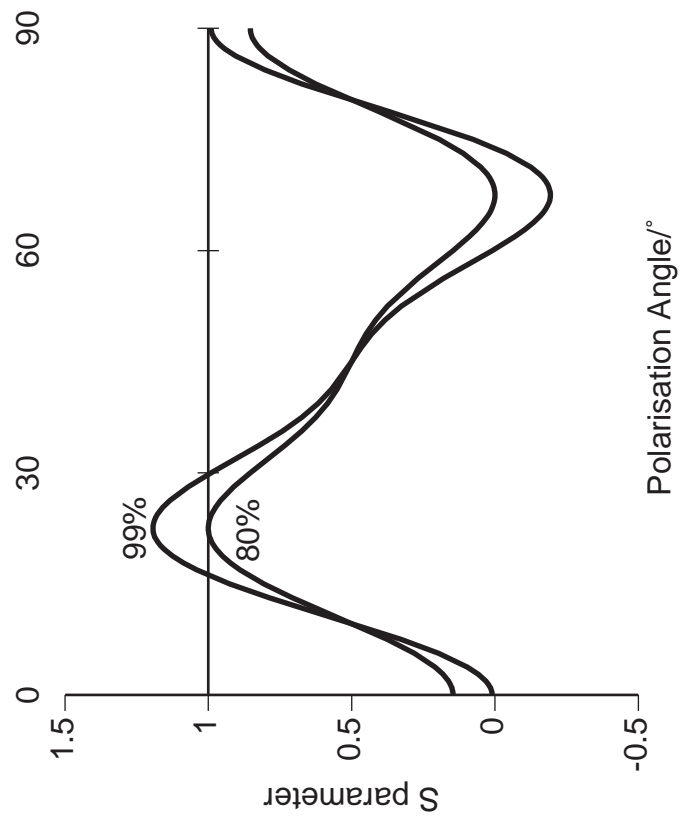
FIG. 2. Schematic of the interferometric modulation system (IMS). The input beam is combined at a beamsplitter with a coherently related local oscillator. The signal from the homodyne detectors is used to modulate the phases of each of the resulting beams, with a  $\pi$  phase shift between them. The beams are then recombined. In the absence of modulation the input emerges unchanged from the output port. The phase modulation couples some of the intensity of the local oscillator into the output beam; in effect the signal is added to the amplitude of the beam.

FIG. 3. The variation of  $S_{A,D'}$  with the polarizer angle ( $\theta_A$ ) at unity gain. The other polarizers are also varied such that the condition  $\theta_A = -\theta_{D'}/2 = \theta'_A/3$  is maintained whilst  $\theta'_{D'} = 0$ . This arrangement maximizes  $S$ . The CH inequality is violated for  $S > 1$ . The two traces are for 99% and 80% squeezing at OPO2.  $\chi_1 = 0.1$

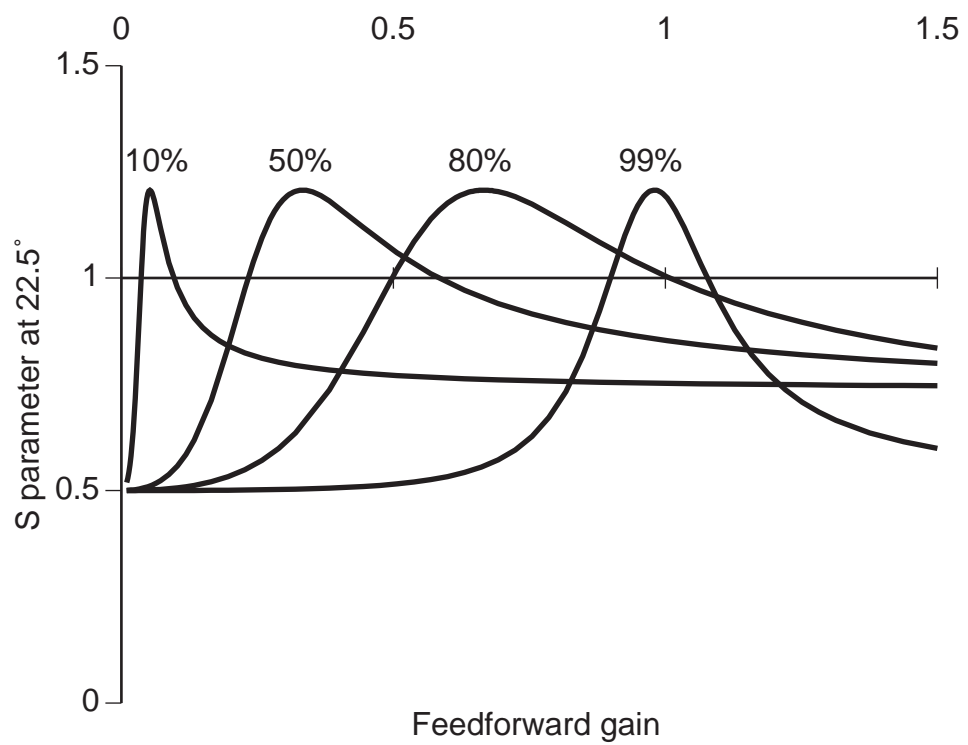
FIG. 4. The variation of  $S_{A,D'}$  with the gain  $\lambda$ , for squeezing of 10%, 50%, 80% and 99%. Each graph has its maximum when  $\lambda = \tanh \chi_2$ , in which case  $S$  has the same value before and after one of the beams is teleported.  $\chi_1 = 0.1$

## REFERENCES

- [1] M. Zukowski, A. Zeilinger, M. A. Horne and A. K. Ekert, Phys. Rev. Lett. **71**, 4287 (1993).
- [2] C. H. Bennett, G. Brassard, C. Crepeau, R. Jozsa, A. Peres and W. K. Wootters, Phys. Rev. Lett. **70**, 1895 (1993).
- [3] S. Bose, V. Vedral and P. L. Knight, Phys. Rev. A **57**, 822 (1998).
- [4] Jian-Wei Pan, Dik Bouwmeester, Harald Weinfurter and Anton Zeilinger, Phys. Rev. Lett. **80**, 3891 (1998).
- [5] L. Vaidman, Phys. Rev. A **49**, 1473 (1994).
- [6] S. L. Braunstein and H. J. Kimble, Phys. Rev. Lett. **80**, 869 (1998).
- [7] A. Furusawa, J. L. Sorensen, S. L. Braunstein, C. A. Fuchs, H. J. Kimble and E. S. Polzik, Science, **282**, 706 (1998).
- [8] P. G. Kwiat, K. Mattle, H. Weinfurter, A. Zeilinger, A. V. Sergienko and Y. Shih, Phys. Rev. Lett. **75**, 4337 (1995).
- [9] J. F. Clauser and M. A. Horne, Phys. Rev. D **10**, 526 (1974).
- [10] S. L. Braunstein and H. J. Kimble, Nature **394**, 840 (1998).
- [11] T. C. Ralph and P. K. Lam, Phys. Rev. Lett. **81**, 5668 (1998).



Polkinghorne et al. Figure 3



Polkinghorne et al. Figure 4